Investigations about periodic design for broadband increased sound transmission loss of sandwich panels using 3D-printed models

F. Errico, M. Ichchou, S. de Rosa, F. Franco, O. Bareille

Investigations about periodic design for broadband increased sound transmission loss of sandwich panels using 3D-printed models

F. Errico[a,b,*], M. Ichchou[a], S. De Rosa[b], F. Franco[b], O. Bareille[a]

[a] *Vibroacoustics & Complex Media Research Group, LTDS-CNRS UMR 5513, Ecole Centrale de Lyon, Écully, 69134, France*
[b] *Pasta-Lab, Dipartimento di Ingegneria Industriale, Universitá degli Studi di Napoli Federico II, Napoli, 80125, Italy*

Abstract

Two types of sandwich panels are designed by using the periodic structure theory. A double-wall panel with mechanical links and a sandwich panel with rectangular core are studied. An oriented optimization of the elastic bending waves' propagation versus the acoustic wavenumbers is achieved by using shifted core walls and by keeping the mass and stiffness of the system constant. Standard and optimized configurations are 3D-printed and sound transmission measurements are carried out by using a facility with an uncoupled reverberant-anechoic configuration. The experimental evidences of enlarged bending band-gaps and deformation mechanisms are proved using a reverse approach based on the acoustic radiation of the panels.

Keywords: Sound Transmission, Periodic Structure Design, Metamaterials, Sandwich Structures

1. Introduction

In transport industry, the requirements for light and stiff structures often lead to sandwich structural solutions. The design of the core of sandwich panels can induce different anisotropies keeping a high stiffness-to-mass ratio. On the other hand, while a reduced mass is an advantage for fixed structural resistance, it generally induces lower vibroacoustic performance. Therefore, the design of sandwich panels for reduced acoustic radiation, limiting the mass of the system, has received more and more attention in the last decades [1, 2, 3, 4].

One of the main reasons for a larger acoustic radiation of sandwich panels is the shear core effect in the mid-frequencies [1, 2, 3, 4, 5, 6]; the transition from global bending to core shear is fundamental [7]. The effects of this wavemode transition has been investigated by describing panel using an equivalent shear core [8, 9, 10].

Some authors tried to design the core geometry in order to optimize the sound transmission. Palumbo et al. [11] and Grosveld et al. [12] proved experimentally the increase of vibroacoustic performance of honeycomb-cored sandwich plates when periodical voids and recesses are included in the original geometry. While this approach creates regions of reduced bending stiffness, a strong benefit is observed in the sound transmission loss for large frequency bands. A brilliant work is

*Corresponding author
Email address: fabrizio.errico@ec-lyon.fr (F. Errico)

also proposed by Hambric et al. in [13] where a complex structural honeycomb panel is optimised by altering the original design, targeting a different the bending wave speed in the media versus the acoustic one.

On the other hand, with the rise of modern numerical techniques as the Wave Finite Element Method (WFEM), detailed investigations on shear-core transitions and the acoustic radiation of sandwich structures, have been conducted. The WFEM, applied also within this work, is used for the dynamic analysis of periodic structures by exploiting the periodic links among neighbouring nodes and substructures [14, 15, 16]. The single elementary cells are modelled instead of the whole panel, without requiring any homogenisation or analytical description of the core.

Baho et al [17], for instance, used a wavemode energy method, coupled with a wave assurance criterion, to predict the transition frequency of honeycomb panels modelled using a single periodic cells. In addition, the core geometry effects on the shear-core transition and sound transmission loss of honeycomb sandwich plates, are investigated in [18]. Zergoune et al. [18] show the transmission loss sensitivity to most of the classic topological parameters of honeycomb cored sandwich panels, such as angles between walls, thickness and deformation of hexagonal core cells.

Similarly, sandwich panels with arbitrary shaped core are studied in [19]. Again, a comparative study of periodic cells that share the same mass-to-stiffness ratio, is performed to achieve a significant variation of the transition frequency and modal density, compared to classic honeycomb.

Alternative approaches, quite efficient when a narrow-band frequency issue has to be solved, are connected to the use of resonant periodically distributed elements [20, 21, 22, 23]. In this case, the drawback is connected to the addition of mass to the structure and to the difficulty in targeting broadband enhancements of the acoustic performance of the panels.

Within the present paper, two common configurations of sandwich panels are modified using the periodic structure theory. The aim is to induce alterations of the bending wave propagation of the panels versus frequency, in order to increase the vibroacoustic performance, keeping the same mass and, optionally, the same bending stiffness as the original designs. A double-wall panel with mechanical links and a sandwich panel with rectangular core are optimised using shifted core walls. In the first case, the periodicity effects are evident and an enlarged band-gap for bending waves is created. In the second case, the main effects are observed on the shear-core transition and core energy absorption through an increased deformation mechanism. All considerations and enhancements are experimentally proved.

It is worth highlight that the optimization proposed here is not connected to any minimization of a specific cost function or parameter; the main idea of the paper is to prove the performance of optimised designs guided by the physical analysis of waves propagation characteristics. A proper topological optimization, exploring a large number of configurations, might lead to different variants of the proposed design, with higher performance.

The paper is organised as follows: Section 2 describes the numerical procedure used for predicting the dispersion curves versus frequency; Section 3 describes the proposed designs; Section 4 describes the experimental set-up used for the measurement of sound transmission loss of the

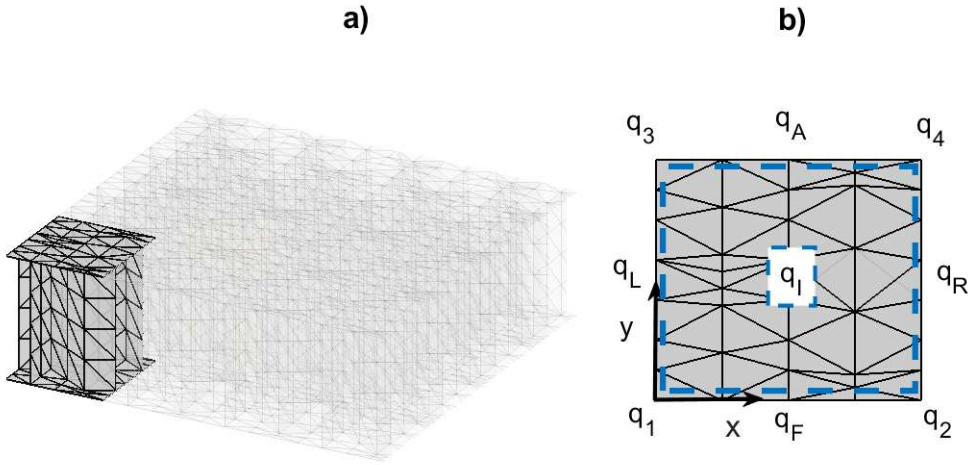

Figure 1: Cell model extracted from a periodic structural system with periodicity along the x-y plane. a) Illustration of a cell within a full FEM model. b) Node ordering following the schemese in Section 2.

3D-printed panels; Section 5 presents the numerical and experimental results.

2. A Numerical Approach for Elastic Waves in a Periodic Media

A free wave propagating along a structure is assumed to take the form of a Bloch wave [14]. Any wavefield in the periodic media is linked with a complex propagation constant, function of the distance among particles. This is physically representative of a magnitude attenuation and phase shift within the periodic structure. This reflects in periodic systems exhibiting passbands and stopbands; i.e. each disturbance can propagate freely only in specific frequency ranges, otherwise they decay with distance [14].

The numerical approach used here to investigate the waves' dispersion in the periodic media is the wave finite element method. It is a FE-based method whose advantage stands in requiring the modelling of a single unit periodic cell, instead of a whole structure (Fig. 1). In fact, by exploiting the links among nodes using complex propagation constants, the dynamics of the whole periodic structural system can be analysed [14, 15, 16].

With reference to Fig. 1, the dynamic stiffness equation of the unitary segment can be written as:

$$\mathbf{D}\mathbf{q} = \mathbf{f} + \mathbf{e}, \tag{1}$$

where $\mathbf{q}$, $\mathbf{f}$ and $\mathbf{e}$ are the vectors of nodal degrees of freedom (DoFs), internal and external forces, respectively; $\mathbf{D}$ is the dynamic stiffness matrix. To analyse the dynamics of the whole periodic system, displacements ($\mathbf{q}$) and forces ($\mathbf{f}$ and $\mathbf{e}$) at any point of the cell can be liked to a reduced subset of degrees of freedom ($\mathbf{q}_r$) by exploiting periodic links, as follows (see Fig. 1 for nodes subsets ordering):

$$\mathbf{q}_A = \mathbf{I}\lambda_Y \mathbf{q}_F; \qquad \mathbf{q}_R = \mathbf{I}\lambda_X \mathbf{q}_L; \qquad \mathbf{q}_2 = \mathbf{I}\lambda_X \mathbf{q}_1; \qquad \mathbf{q}_3 = \mathbf{I}\lambda_Y \mathbf{q}_1; \qquad \mathbf{q}_4 = \mathbf{I}\lambda_X \lambda_Y \mathbf{q}_1; \tag{2}$$

being the propagation constants:

$$\lambda_X = \mathrm{e}^{-\mathrm{i}k_X L_X}, \qquad \lambda_Y = \mathrm{e}^{-\mathrm{i}k_Y L_Y}, \tag{3}$$

where k_X and k_Y are wavenumbers of the waves in the plane $x-y$; L_X and L_Y represent the cell lengths along the same directions, respectively, and $\mathbf{I}$ is the identity matrix.

For complex structures requiring a fine mesh, a modal reduction is highly suggested to reduce the order of the model. The displacement vector inside a single unit cell can be substituted by a subset of stationary constrained internal modes, achieving a significant reduction of the number of inner DOFs. The displacements vector can be expressed as in Eq. 4, using a projection matrix ($\mathbf{G}$) that includes static boundary modes ($\mathbf{\Psi}_B$) and component modes ($\mathbf{\Psi}_C$):

$$\begin{bmatrix} \mathbf{q}_{nI} \\ \mathbf{q}_I \end{bmatrix} = \mathbf{G} \begin{bmatrix} \mathbf{q}_{nI} \\ \mathbf{P}_{mod} \end{bmatrix}; \qquad \mathbf{G} = \begin{bmatrix} \mathbf{I} & \mathbf{0} \\ \mathbf{\Psi}_B & \mathbf{\Psi}_C \end{bmatrix} \tag{4}$$

where $\mathbf{P}_{mod}$ represents modal participation factors vector for the set of retained modes; $\mathbf{q}_{nI}$ is the whole set of degrees of freedom excluded the ones belonging to the internal nodes. The static boundary modes $\mathbf{\Psi}_B$ and component modes $\mathbf{\Psi}_C$ can be derived as in a Craig-Bampton (CB) framework [24, 25]. Finally the stiffness and mass matrices of the condensed system can be calculated by pre and post multiplying for the projection matrix $\mathbf{G}$, defined in Eq. 4:

$$\mathbf{M}_\mathrm{C} = \mathbf{G}^\mathrm{T}\mathbf{M}\mathbf{G}; \qquad \mathbf{K}_\mathrm{C} = \mathbf{G}^\mathrm{T}\mathbf{K}\mathbf{G}, \tag{5}$$

where the subscript C refers to the mass and stiffness matrices of the cell being condensed. Then, at each frequency step, the modal participation factors can be statically condensed and the condensed dynamic stiffness equation $\mathbf{D}_C$ obtained [24, 25]. Assembling the links in Eq. 2 in a global periodicity matrix $\mathbf{\Lambda}$ and pre-multiplying Eq.1 by the Hermitian of this matrix, a reduced dynamic stiffness equation can be written:

$$\mathbf{D}_r\mathbf{q}_r = \mathbf{\Lambda}^\mathrm{H}[\mathbf{D}_C]\mathbf{\Lambda}\mathbf{q}_r = \mathbf{\Lambda}^\mathrm{H}\mathbf{\Lambda}\mathbf{f}_r + \mathbf{\Lambda}^\mathrm{H}\mathbf{\Lambda}\mathbf{e}_r. \tag{6}$$

where $\mathbf{D}_r$ is the dynamic stiffness matrix of the reduced model; $\mathbf{q}_r$, $\mathbf{f}_r$ and $\mathbf{e}_r$ are the displacements, internal forces and external forces of the reduced model, respectively. Given the equilibrium of the internal forces between consecutive cells, only potential external forces are considered [16], thus $\mathbf{\Lambda}^\mathrm{H}\mathbf{\Lambda}\mathbf{f}_r = 0$.

The problem in Eq. 6 is a three-parameters eigenproblem in ω, λ_X and λ_Y, whose eigenvectors and eigenvalues are the propagating wavemodes and the corresponding constants of propagation. It is here solved by imposing the frequency and one wavenumber to zero, in order to study singularly the wave propagation in x and y directions.

3. Shifted-Walls Design

A core design with shifted walls is here proposed for two common types of sandwich panels.

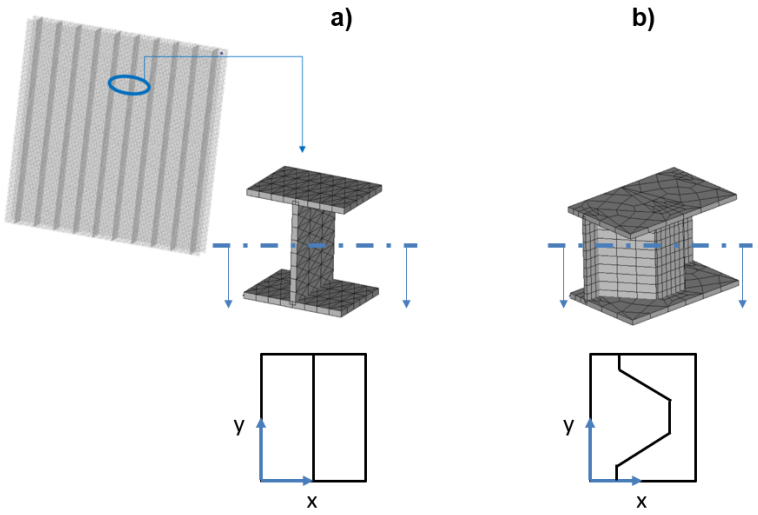

Figure 2: Cell models extracted from a Double-Wall Panel with Mechanical links. a) Standard design. b) Proposed Optimal Design.

First a double-wall panel with rectilinear mechanical links (Fig. 2a) is analysed for a trapezoidal shape of the stiffener (Fig. 2b). A similar idea has been applied to a sandwich panel with rectangular core (Fig. 5a), where the core walls have been folded in one direction (Fig. 5b).

The frequency band targeted for the optimization is 250 Hz to 10 kHz, corresponding to the measurements frequency range available for the facility used within this work (see Sec. 4).

3.1. Double-Wall Panel with Mechanical Links

The initial double-wall panel (Fig. 2a) is 1.06 cm thick (total thickness) and has a 1.0 cm spacing between consecutive stiffeners, in the periodicity direction (axis x in Fig. 2). The thickness of the skins and core walls is 0.6 mm. A unit cell, as the one illustrated in Fig. 2a, is modelled with finite elements (ANSYS Shell181) and the eigenvalue problem developed in Section 2 solved to get the wave dispersion in the media.

Full geometrical details for the designs analysed are given: the double wall panel with mechanical link is illustrated in Fig. 3, while the sandwich panel with rectangular core is illustrated in Fig. 4.

The modified design, proposed here for increasing the flexural band-gap region versus frequency, in the periodicity direction, is characterised by a trapezoidal (top-view) shape of the stiffer (Fig. 2b). The same global thickness and stiffeners' spacing as the classic double-wall panel is used; the skins are 0.6 mm-thick and the core walls are 0.45 mm-thick, in order to keep the same mass of the system.

The idea of using such a geometrical shape comes from the usually low bending and shear stiffness of this kind of panels in the direction normal to the stiffener envelope (axis x). The addition of oblique elements, periodically repeated in the x-y plane due to the periodicity of the system, has a main function: the core shear stiffness increases with respect to the classic design

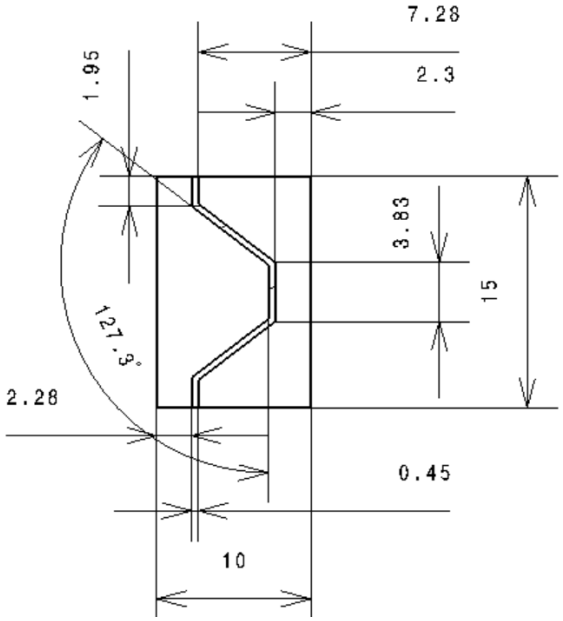

Figure 3: Cell model extracted from the optimized double-wall panel with mechanical links. Distances in millimetres.

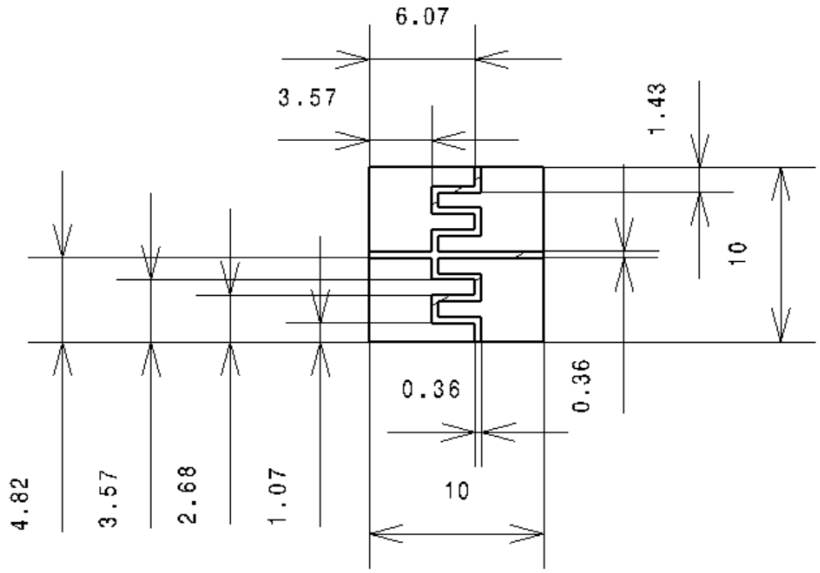

Figure 4: Cell model extracted from the optimized sandwich panel with rectangular core. Distances in millimetres.

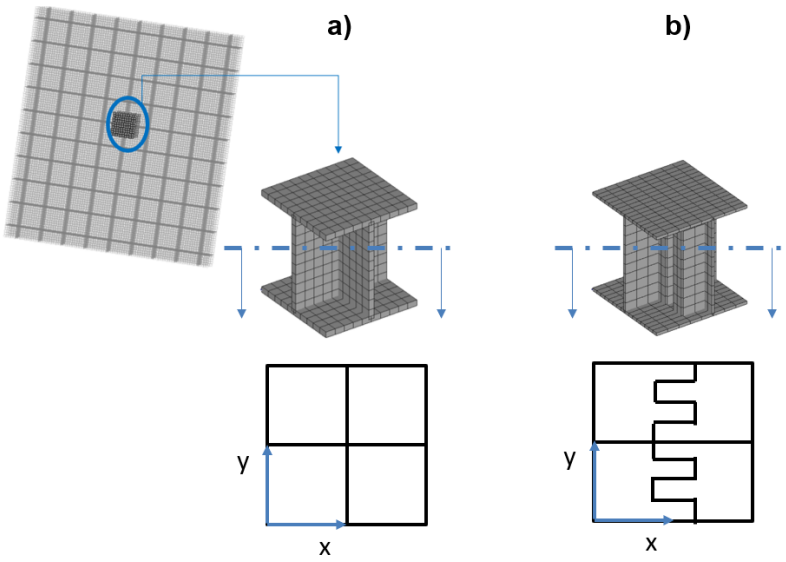

Figure 5: Cell models extracted from a Sandwich Panel with Rectangular Core. a) Standard design. b) Proposed Optimal Design with shifted walls.

where the bending of the mechanical link was proving the whole core-shear stiffness in the x direction.

3.2. Rectangular-Core Panel

For the rectangular-cored panel, the initial design (Fig. 5a) has a total thickness of 1.06 cm and a 1.0 cm spacing between consecutive stiffeners, in both directions (Fig. 5a). As for the double-wall panel, both skins and core-walls are 0.6 mm-thick. Similarly to the previous case, the modified design proposed here is characterised by a trapezoidal (top-view) shape of the stiffener in one direction (axis y in Fig. 5b), while the rectilinear geometry is kept in the other direction. To keep the same mass, global thickness and stiffeners spacing of the original system, the skins are 0.6 mm-thick and the core walls are 0.36 mm-thick. Hereby, the target is to tailor the elastic waves dispersion in the panel, against the acoustic wavenumbers. Differently from the previous case, the presence of additional components of the stiffener in the x direction (Fig. 5b) does not have the function of increasing the core-shear stiffness. The idea is to induce a larger deformation mechanism for the folded core walls both for bending in y and core-shear in x.

4. Experimental Set-Up

The work flow followed for the analysis and testing of the presented design configurations is illustrated in Fig. 6. Using the method described in Section 2, the numerical dispersion curves and transmission loss are computed and compared. Then, a CAD model is developed and transformed into a CAM input file for a Stratasys $Fortus$ 450mc industrial 3D-printer with a maximum printable volume of 40 x 35 x 40 cm^3 (Fig. 6). The material used for the modelling and 3D-printing of

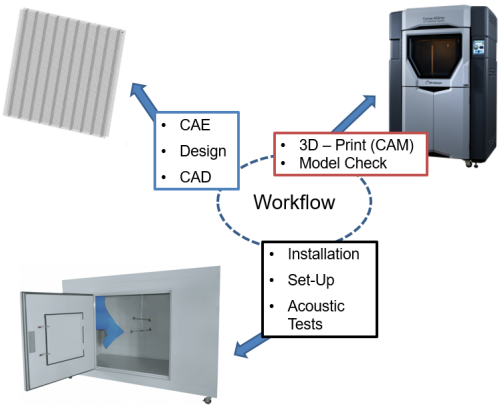

Figure 6: Work-flow scheme for panel design optimisation based on numerical and experimental data.

the panels is the ABS-M30 (Acrylonitrile butadiene styrene) [26]. The material has been experimentally characterised and has the following properties: E = 1.8 GPa; $\rho = 988$ kg/m^2; $\nu = 0.32$. Both the 3D-printed panels with standard and optimised designs are shown in Fig. 8.

The sound transmission measurements were performed in an un-coupled reverberant-anechoic room as in Fig. 7. The reverberant room has volume of 2.50 x 1.40 x 1.75 m^3 and reflective surfaces are installed inside to increase the diffusiveness of the reverberant room; the calculated Schroeder frequency is $\approx$ 600 kHz [27]. The acoustic excitation is generated using four speakers installed at the four top corners of the reverberant room, with an uncorrelated white noise input from 50 to 10 kHz.

The transmitted sound power is measured using a Bruel & Kjaer sound intensity probe with two half-inch microphones and a 6.0 mm spacer (see Fig. 7). The incident sound power is obtained by the sound pressure level measurements in the cabin room, averaged among four half-inch microphones disposed as in Fig. 7. The anechoic conditions of the receiving room are simulated by covering the room walls with absorbing layers, whose distance from the tested panel is larger than 2 m. The sound transmission loss (TL) is finally calculated, assuming that the excited and radiating surfaces are the same, as:

$$\mathrm{TL} = L_p - L_i - 6.18, \tag{7}$$

where L_p is the average pressure level measured in the reverberant room, L_i the average sound intensity level over the surface of the test-panels in the semi-anechoic room, while the -6.18 factor arises from reference values in dB conversion [28].

5. Results

5.1. Waves Tailoring versus Acoustic Wavenumbers

The approach presented in Section 2 is used for studying the waves' propagation in the periodic structures proposed in Section 3. The main idea is to evidence two phenomena: an increase of the bending band-gap in the periodicity direction, for the double-wall panel with mechanical links; an

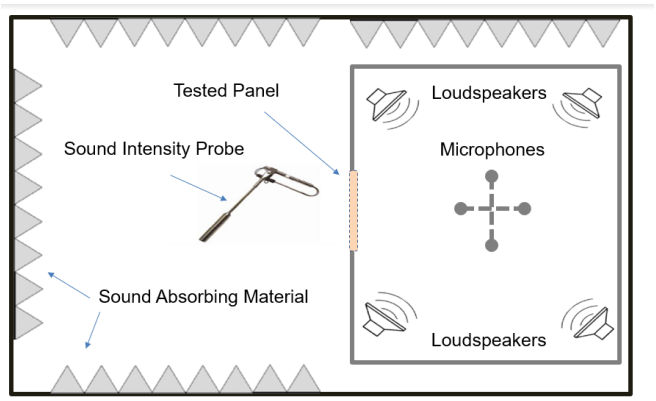

Figure 7: Illustration of the test facility with un-coupled reverberant-anechoic rooms for transmission loss measurements.

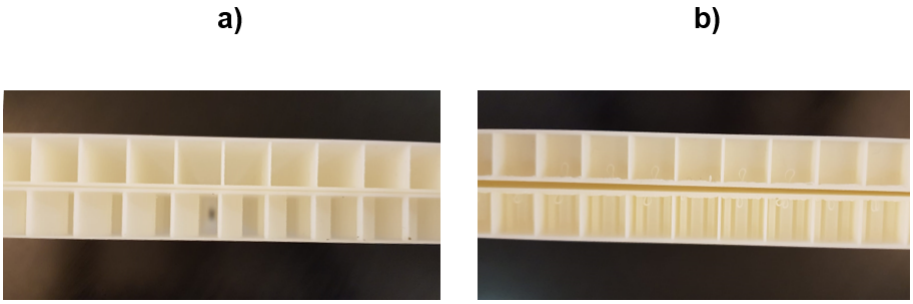

Figure 8: The 3D-printed panels side-view following the standard (up) and optimised(down) designs in: a) Fig. 2 - Double-Wall panel with mechanical links; b) Fig. 5 - Sandwich panel with rectangular core.

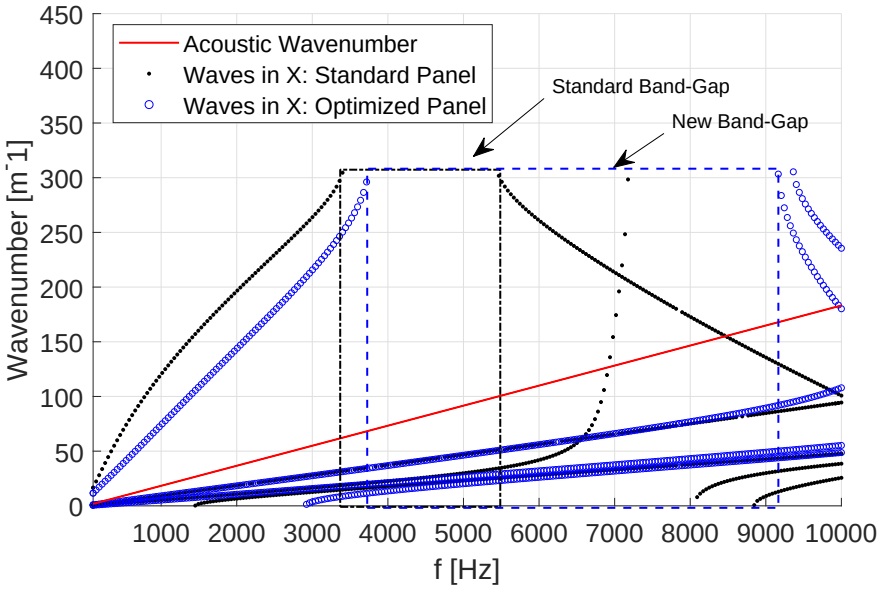

Figure 9: Dispersion Curves of the Double-Wall Panel designs; eigenvalue solutions of the eigenvalue problem in Eq. 6.

increase of bending wavenumbers versus the acoustic ones, for the sandwich panel with rectangular core.

In Fig. 9, the dispersion curves for the two designs illustrated in Fig. 2 are compared in the direction orthogonal to the stiffening elements. The band-gap present in the standard design extends from 3.3 kHz to 5.4 kHz and an acoustic coincidence is observed around 8.4 kHz. Differently, for the optimized design proposed in Fig. 2, the band-gap is strongly enlarged in frequency from 3.6 kHz to 9.1 kHz, while a coincidence is observed only at the end of the frequency band of interest ($\approx$ 10 kHz). A double advantage is thus observed both in structural waves' filtering (band-gap) and coincidence shift, keeping the same mass of the system.

In Fig. 10 the eigenvectors of Eq. 6, which represent wavemodes of the wave-type propagating in the media with the wavenumbers of Fig. 9, are showed for two frequencies. In particular, the wavemodes with the highest wavenumbers of the set of waves propagating at 4.5 kHz and 6.5 kHz are shown for the two designs in Fig. 2. It is interesting to observe how, in Fig. 10, the cell modal wave deformations are completely different. The increase of core-shear stiffness in the periodicity direction, for the optimized design, induces almost null modal out-of-plane displacements of the skin surfaces. In opposition, the wavemodes of the classic design still present mode-shapes efficient for sound transmission (non-null out-of-plane displacements).

Differently, for the classic sandwich panel with rectangular core, band-gaps are not present in the frequency range of interest (see Fig. 11). Here, a coincidence effect is not observed, but the bending waves follow closely and almost parallel the acoustic wavenumbers versus frequency. This means that the sound transmission loss is expected to be reduced in a large frequency bandwidth.

The target of the optimised design, in this case, has been to enlarge the distance between the

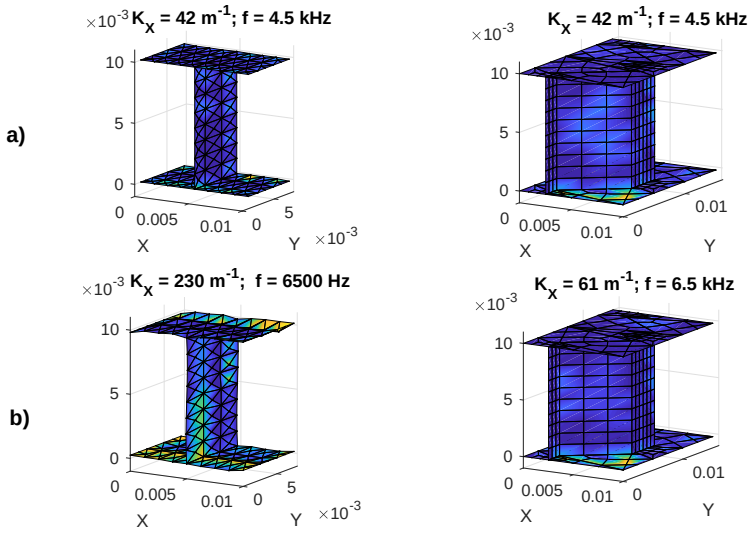

Figure 10: Wavemodes of the Double-Wall Panel designs for waves propagating in x direction; eigenvector solutions of the eigenvalue problem in Eq. 6. a) f = 4.5 kHz; b) f = 6.5 kHz.

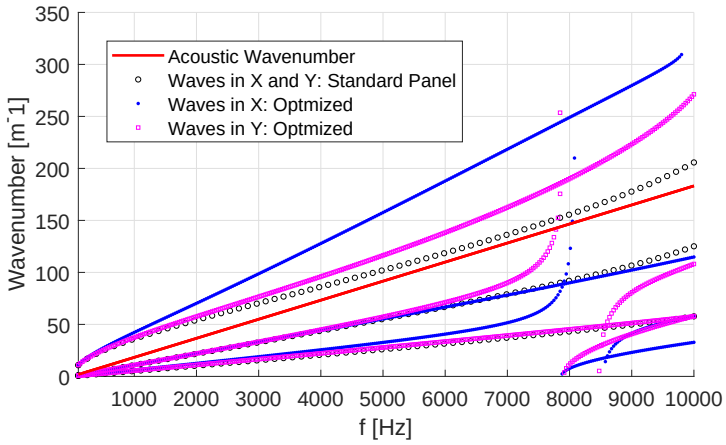

Figure 11: Dispersion Curves of the Sandwich Panel with Rectangular core designs; eigenvalue solutions of the eigenvalue problem in Eq. 6.

structural and acoustic wavenumbers for a large frequency band, by inducing a larger deformation mechanism of the folded core walls. Coherently, in Fig. 11, the waves' dispersion, both in x and y directions, is characterised by higher wavenumbers: the larger distance from the acoustic ones is expected to induce an enhanced sound transmission loss. In addition, a band-gap formation in x, at the end of the frequency band, is also observed for the optimised design. The wave shapes in x (wavemodes) at 4 and 6 kHz are presented in Fig. 12 for bending waves. As said before, the folded walls design offers a larger core deformation mechanism and this is clearly observable in Fig. 12 for both frequencies: a part of the vibrational energy is absorbed through the core deformation. In this way, the shear core waves reduce their speed and the corresponding wavenumbers increase, as targeted.

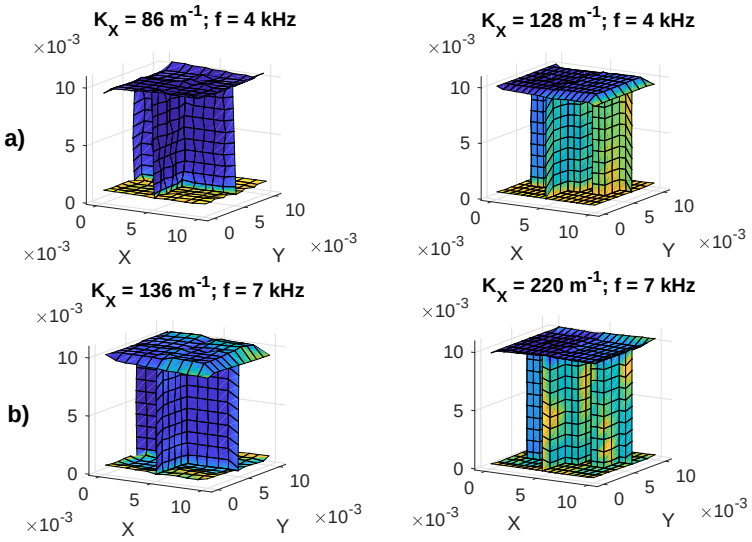

Figure 12: Wavemodes of the Sandwich Panel with Rectangular core designs for waves propagating in x direction; eigenvector solutions of the eigenvalue problem in Eq. 6. a) f = 4.0 kHz; b) f = 6.0 kHz

5.2. Sound Transmission Loss

The sound transmission loss of the two couples of designs is numerically simulated for equivalent infinite panels.

The effects of the design optimisation, observed in terms of waves in Figs. 9 and 11, are specular in the transmission loss curves presented in Fig. 13. In Fig. 13a, the double-wall panel with mechanical links is studied and the effect of the enlarged band-gap effect is visible in shifting the coincidence frequency: starting from 1.5kHz, the sound transmission loss of the optimised panel is constantly larger than the one of the standard plate design with the same mass.

On the other hand, in Fig. 13b, as observed from the dispersion curves, while a real coincidence region is not observed for the standard sandwich plate design, a drop of the transmission loss is still evident due to the proximity of the structural and acoustic wavenumbers/wavelengths. Differently, for the optimised design, the induced distance of structural and acoustic wavenumber results in a constant increase of the sound transmission loss versus frequency, in absence of evident drops: from 1.5 kHz to 10 kHz, the new design assures a larger sound transmission loss with the same global mass of the panel.

To experimentally prove the increase of sound transmission loss for the proposed designs, the 3D-printed panels are installed and clamped in the TL facility, as in Fig. 7. The expected and real weights of the printed panels are reported in Table 1. It is observed in Table 1 that, when the geometrical complexity of the single cell design increases (optimised designs), the discrepancies between the expected and real weight of the 3D-printed panels increases too. To compare mass-normalised results, the approach proposed by De Rosa in [29] is used to scale the measured transmission loss curves of the optimised panels versus the ones of the lighter (standard; see Table 1) panels.

In Fig. 14, the measured sound transmission losses (mass-normalised) of the two design couples

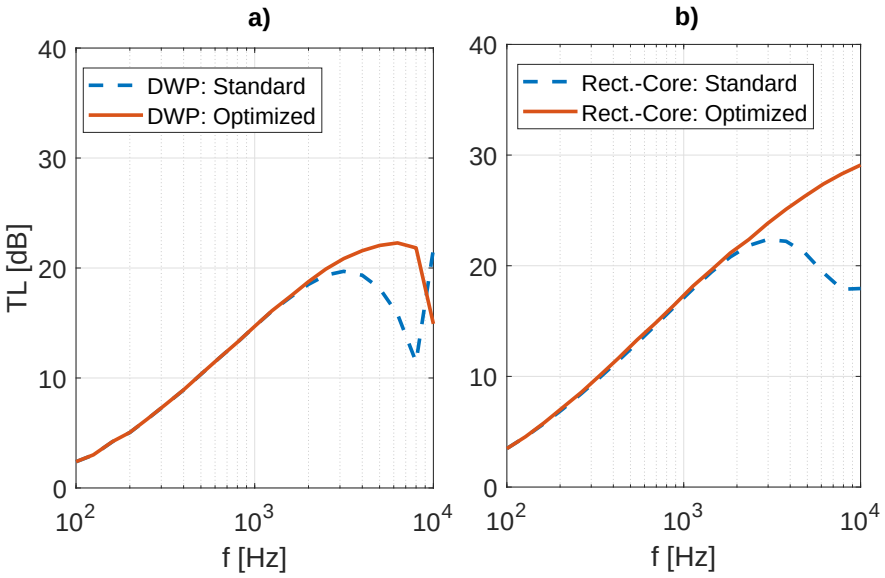

Figure 13: Calculated Transmission Loss for infinite panels the proposed designs. a) Double-Wall panels designs; b) Rectangular-Cored Sandwich panel designs.

Table 1: Expected and Measured weights of the 3D-printed panels

	Expected [gr]	Measured [gr]	Difference [%]
Standard (Fig. 2a)	246	245	- 0.4
Optimised (Fig. 2b)	246	287	+ 16.6
Standard (Fig. 5a)	341	346	+ 1.4
Optimised (Fig. 5b)	342	360	+ 5.3

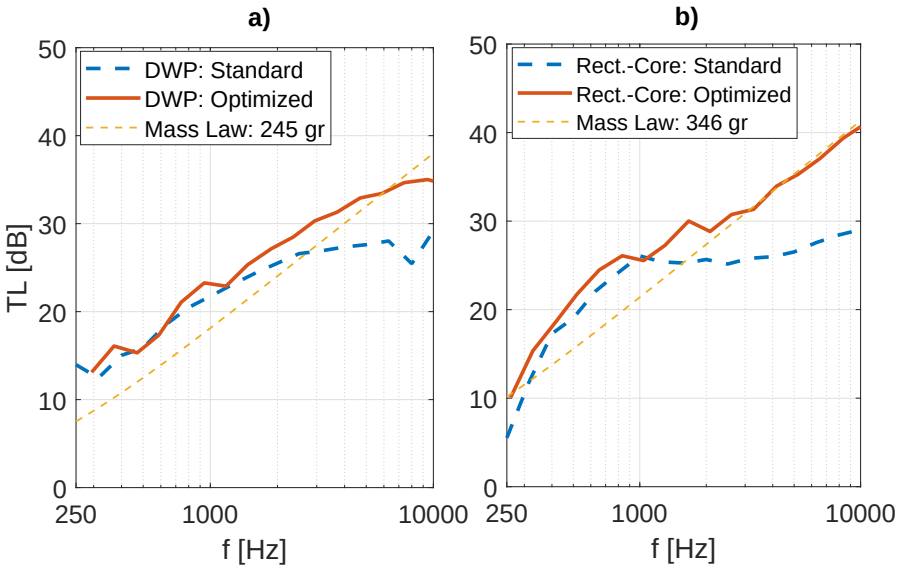

Figure 14: Measured Transmission Loss (mass-normalised) for the 3D-printed panels. Total panel surface: 0.40x0.35 m^2. Exposed panel surface: 0.34x0.29 m^2. a) Double-Wall panels designs; b) Rectangular-Cored Sandwich panel designs.

proposed in Section 3 are compared. While the total surface of the plates is 0.40 x 0.35 m^2, the exposed panel surface is 0.34 x 0.29 m^2. In Fig. 14a, the measured sound transmission loss trends are in good agreement to the simulated ones for an equivalent infinite plate in Fig. 13a: as expected, the increase of sound transmission loss starts from 1.5 kHz and continues up to the end of the frequency band of interest. It must be highlighted that the damping induced by the 3D-printing, the installation and the clamping in the TL cabin might be high. It is also observed by the measured transmission loss curve around the coincidence region ($\approx$ 8.4 kHz) for the standard DWP in Fig. 14a, with respect to the simulated drop in Fig. 13a.

Similarly, in Fig. 14b, the same trends of the simulation Fig. 13b, for the sandwich plate with rectangular core, are experimentally observed. Again, the reduction of transmission loss expected for the standard design is highly damped with respect to the simulation. However, the agreements is satisfying and validates the expected trends. The increase of sound transmission loss, as in the previous case, appears in a very large frequency band that goes from 1 kHz to 10 kHz, at least, for a fixed mass of the panel.

Although there is a general agreement between expected results and experimental evidence, some discrepancies are present. For example, in both cases the sound transmission loss increase starts in frequencies a bit lower than the expected ones. This should be addressed to two factor that act simultaneously.

First, as discussed before, the Schroeder frequency of the TL cabin is $\approx$ 600 kHz and this can have an influence on the reliability of the measurements in the low frequency bands. Furthermore, the uncertainties connected to the 3D-printing and the effective differences among the ideal models and the real structures are not perfectly controlled and might, obviously, induce discrepancies by

the predictions and the measurements.

6. Concluding Remarks

Two types of sandwich panels are analysed in terms of waves' propagation and sound transmission loss by using periodic structure theory. A double-wall panel with mechanical links and a sandwich panel with rectangular core are considered. A core optimization using shifted core walls is proposed targeting the structural waves' propagation versus the acoustic wavenumbers, forcing the mass to be fixed to the value of the original designs.For the double-wall panel with mechanical links an enlarged bending band-gap is achieved in a large frequency band, shifting the acoustic coincidence almost out of the frequency band of interest. For the sandwich panel with rectangular core, an increased core deformation mechanisms is achieved distancing the structural(bending) and acoustic wavenumbers versus frequency.

Standard and optimized configurations are 3D-printed and sound transmission loss measurements are carried out using a small facility with uncoupled reverberant and semi-anechoic configuration.

Numerical simulations and experimental tests evidence an increased vibro-acoustic performance of the new designs. The transmission loss measurements showed that, even keeping the same total mass of the panels, the sound transmission loss is increased in a very large frequency band that goes from $\approx$ 1.5 kHz to 10 kHz.

Acknowledgments

This project has received funding from the European Unions Horizon 2020 research and innovation programme under the Marie Sklodowska-Curie grant agreement No. 675441. Nassardin Guenfoud, Benoit Minard and Stephane Lemahieu, from Ecole Centrale de Lyon, are gratefully acknowledged for the help in 3D-printing and building the adaptive clamping system of the cabin.

References

[1] M. A. Lang, C. L. Dym, Optimal acoustic design of sandwich panels, The Journal of the Acoustical Society of America 57 (6) (1975) 1481–1487. doi:10.1121/1.380588.
URL https://doi.org/10.1121/1.380588

[2] J. A. Moore, R. H. Lyon, Sound transmission loss characteristics of sandwich panel constructions, The Journal of the Acoustical Society of America 89 (2) (1991) 777–791. doi:10.1121/1.1894638.
URL https://doi.org/10.1121/1.1894638

[3] C. L. Dym, C. S. Ventres, M. A. Lang, Transmission of sound through sandwich panels: A reconsideration, The Journal of the Acoustical Society of America 59 (2) (1976) 364–367. doi:10.1121/1.380871.
URL https://doi.org/10.1121/1.380871

[4] C. L. Dym, M. A. Lang, Transmission of sound through sandwich panels, The Journal of the Acoustical Society of America 56 (5) (1974) 1523–1532. doi:10.1121/1.1903474.
URL https://doi.org/10.1121/1.1903474

[5] G. Kurtze, B. G. Watters, New wall design for high transmission loss or high damping, The Journal of the Acoustical Society of America 31 (6) (1959) 739–748. doi:10.1121/1.1907780.
URL https://doi.org/10.1121/1.1907780

[6] F. Franco, K. A. Cunefare, M. Ruzzene, Structural-acoustic optimization of sandwich panels, ASME J. Vib. Acoust 129 (3) (2006) 330–340. doi:/10.1115/1.2731410.

[7] F. J. Fahy, P. Gardonio, Sound and structural vibration: radiation, transmission and response, Elsevier, 2007.

[8] B. Clarkson, M. Ranky, Modal density of honeycomb plates, Journal of Sound and Vibration 91 (1) (1983) 103 – 118. doi:https://doi.org/10.1016/0022-460X(83)90454-6.
URL http://www.sciencedirect.com/science/article/pii/0022460X83904546

[9] J. Han, K. Yu, X. Li, R. Zhao, Modal density of sandwich panels based on an improved ordinary sandwich panel theory, Composite Structures 131 (2015) 927 – 938. doi:https://doi.org/10.1016/j.compstruct.2015.06.039.
URL http://www.sciencedirect.com/science/article/pii/S0263822315005036

[10] K. Renji, P. Nair, S. Narayanan, Modal density of composite honeycomb sandwich panels, Journal of Sound and Vibration 195 (5) (1996) 687 – 699. doi:https://doi.org/10.1006/jsvi.1996.0456.
URL http://www.sciencedirect.com/science/article/pii/S0022460X96904563

[11] D. L. Palumbo, J. Klos, Development of quiet honeycomb panels, Virginia, Langley Research Center; NASA/TM-2009-215954 (2009).

[12] F. W. Grosveld, D. L. Palumbo, J. Klos, W. D. Castle, Finite element development of honeycomb panel configurations with improved transmission loss, INTER-NOISE 2006 - 35th International Congress and Exposition on Noise Control Engineering; 3-6 Dec. 2006; Honolulu, HI; United States (2006).

[13] S. Hambric, M. Shepherd, K. Koudela, D. Wess, R. Snider, C. May, P. Kendrick, E. Lee, L.-W. Cai, Acoustically tailored composite rotorcraft fuselage panels, Virginia, Langley Research Center; NASA/CR2015-218769 (2015).

[14] L. Brillouin, Wave propagation in periodic structures: Electric filters and crystal lattices, 2nd edition Dover Publications (Mineola, New York). doi:10.1016/S0031-8914(53)80099-6.

[15] D. Mead, Wave propagation in continuous periodic structures: research contributions from southampton, Journal of Sound and Vibration 190 (3) (1996) 495–524. doi:/10.1006/jsvi.1996.0076.

[16] E. Manconi, B. R. Mace, Modelling wave propagation in two dimensional structures using finite element analysis, Journal of Sound and Vibration 318(45) (2008) 884–902. doi:/10.1016/j.jsv.2008.04.039.

[17] O. Baho, Z. Zergoune, M. Ichchou, B. Harras, R. Benamar, B. Troclet, O. Bareille, On global bendingshear core transition effects for the vibroacoustic of sandwich structures: Analytical and numerical investigations, Composite Structures 154 (2016) 453 – 463. doi:https://doi.org/10.1016/j.compstruct.2016.07.062.
URL http://www.sciencedirect.com/science/article/pii/S0263822316312909

[18] Z. Zergoune, M. Ichchou, O. Bareille, B. Harras, R. Benamar, B. Troclet, Assessments of shear core effects on sound transmission loss through sandwich panels using a two-scale approach, Computers & Structures 182 (2017) 227 – 237. doi:https://doi.org/10.1016/j.compstruc.2016.11.017.
URL http://www.sciencedirect.com/science/article/pii/S0045794916304217

[19] C. Droz, Z. Zergoune, R. Boukadia, O. Bareille, M. Ichchou, Vibro-acoustic optimisation of sandwich panels using the wave/finite element method, Composite Structures 156 (2016) 108 – 114, 70th Anniversary of Professor J. N. Reddy. doi:https://doi.org/10.1016/j.compstruct.2016.01.025.
URL http://www.sciencedirect.com/science/article/pii/S0263822316000386

[20] C. Claeys, P. Sas, W. Desmet, On the acoustic radiation efficiency of local resonance based stop band materials, Journal of Sound and Vibration 333 (14) (2014) 3203 – 3213. doi:https://doi.org/10.1016/j.jsv.2014.03.019.
URL http://www.sciencedirect.com/science/article/pii/S0022460X14001990

[21] C. Claeys, K. Vergote, P. Sas, W. Desmet, On the potential of tuned resonators to obtain low-frequency vibrational stop bands in periodic panels, Journal of Sound and Vibration 332 (6) (2013) 1418 – 1436. doi:https://doi.org/10.1016/j.jsv.2012.09.047.
URL http://www.sciencedirect.com/science/article/pii/S0022460X1200853X

[22] Z. Liu, R. Rumpler, L. Feng, Broadband locally resonant metamaterial sandwich plate for improved noise insulation in the coincidence region, Composite Structures 200 (2018) 165 – 172. doi:https://doi.org/10.1016/j.compstruct.2018.05.033.
URL http://www.sciencedirect.com/science/article/pii/S0263822318303520

[23] Z. Liu, R. Rumpler, L. Feng, Investigation of the sound transmission through a locally resonant metamaterial cylindrical shell in the ring frequency region, Journal of Applied Physics 125 (11) (2019) 115105. doi:10.1063/1.5081134.

[24] C. Zhou, J.-P. Laine, M. Ichchou, A. Zine, Wave finite element method based on reduced model for one-dimensional periodic structures, International Journal of Applied Mechanics 7 (2) (2015) 32–47. doi:/10.1142/S1758825115500180.

[25] C. Zhou, J. Lain, M. Ichchou, A. Zine, Multi-scale modelling for two-dimensional periodic structures using a combined mode/wave based approach, Computers & Structures 154 (2015) 145 – 162. doi:https://doi.org/10.1016/j.compstruc.2015.03.006.
URL http://www.sciencedirect.com/science/article/pii/S0045794915000887

[26] D. Croccolo, M. D. Agostinis, G. Olmi, Experimental characterization and analytical modelling of the mechanical behaviour of fused deposition processed parts made of abs-m30, Computational Materials Science 79 (2013) 506 – 518. doi:/10.1016/j.commatsci.2013.06.041.
URL http://www.sciencedirect.com/science/article/pii/S0927025613003741

[27] M. R. Schroeder, The Schroeder frequency revisited, The Journal of the Acoustical Society of America 99 (5) (1996) 3240–3241. doi:/10.1121/1.4148682.

[28] A. London, Transmission of Reverberant Sound Through Single Walls, Department of Commerce National Bureau of Standard, Part of the Journal of Research of the National Bureau of Standards 42, Vol. 42, 1949.

[29] S. D. Rosa, M. Capobianco, G. Nappo, G. Pagnozzi, Models and comparisons for the evaluation of the sound transmission loss of panels, Proceedings of the Institution of Mechanical Engineers, Part C: Journal of Mechanical Engineering Science 228 (18) (2014) 3343–3355. doi:10.1177/0954406214530597.
URL https://doi.org/10.1177/0954406214530597